Abdominal Radiology

Published online: 8 September 2018

Abdom Radiol (2019) 44:669–684
https://doi.org/10.1007/s00261-018-1755-1

Magnetic resonance imaging of the placenta and gravid uterus: a pictorial essay

Daniel C. Oppenheimer,[1] Parisa Mazaheri,[2] David H. Ballard,[2] Motoyo Yano,[2] and Kathryn J. Fowler[2]

[1]Department of Imaging Sciences, University of Rochester Medical Center, 601 Elmwood Ave, P.O. Box no. 648, Rochester, NY 14642, USA

[2]Mallinckrodt Institute of Radiology, Washington University School of Medicine, 510 S. Kingshighway Blvd, St. Louis, MO 63110, USA

Abstract

The placenta is commonly overlooked on magnetic resonance imaging of the pregnant patient, which is frequently performed for alternative reasons such as to characterize fetal or uterine anomalies or to investigate the etiology of acute pelvic pain in pregnancy. Placental disorders have potential for significant maternal and fetal morbidity and peripartum complications if not recognized and treated in a timely manner. The radiologist must be familiar with normal placental variants and the spectrum of benign to life-threatening conditions affecting the placenta so that the Obstetrician can be promptly notified and patient management altered, if necessary. In this pictorial essay, we will describe our MR protocol for placental imaging, provide an image-rich review of the normal placenta, placental variants, and a variety of pathological conditions affecting the placenta and gravid uterus.

Key words: Placenta—Pregnancy imaging—Magnetic resonance imaging—Placenta accreta

Ultrasound (US) is the primary imaging modality used for antepartum fetal imaging because it can detect fetal and placental abnormalities, lacks ionizing radiation, has widespread availability, and can be repeated over the course of the pregnancy with minimal risk to the patient and fetus [1]. Magnetic resonance (MR) imaging offers many advantages to US, including superior soft tissue contrast resolution as well as advanced fetal imaging techniques such as arterial spin labeling. MR is being performed with increasing frequency in the prenatal setting to evaluate fetal and maternal pathologies. The purpose of this pictorial essay is to describe the MR imaging techniques and findings of various conditions which affect the placenta and gravid uterus.

Correspondence to: Daniel C. Oppenheimer; *email:* Daniel_Oppenheimer@URMC.Rochester.edu

Placental imaging modalities

While US is the first line modality for detecting fetal and placental abnormalities, it may be limited by poor acoustic windows, overlying bowel gas obscuring structures of interest and a small field of view. MR provides improved soft tissue contrast compared with US, but it may be limited by patient claustrophobia, cost, and availability in remote or underserved locations. Supine imaging in the MR bore is generally well tolerated in the second trimester, but decubitus positioning may be necessary for patients in the third trimester due to patient discomfort from the gravid uterus when laying supine.

Many investigators have evaluated the safety of MR in the pregnant patient, and there is no conclusive evidence of any deleterious effects of MR imaging on the developing fetus at 1.5T [2–4]. In addition, while there is less information regarding MR safety at higher field strength, the available evidence suggests there are no reproducible harmful effects to the fetus at MR field strength of 3T [2, 3]. MR Imaging at 3T provides higher signal-to-noise ratio (SNR) and decreases the scan time, but also increases absorption rate (SAR) as well as susceptibility and chemical shift artifacts and dielectric effects. The potential effects of time varying gradient and radiofrequency magnetic fields on the fetus are unknown, and these theoretical risks should be carefully considered in all pregnant patients on an individual basis [3, 5].

Gadolinium-based contrast should not be routinely administered to pregnant patients, but its use may be considered in rare instances following careful discussion between the radiology and clinical teams and after

obtaining informed consent from the patient [6]. Gadolinium-based contrast agents are classified as class C (adverse effects on the fetus in animal studies, no well-controlled studies in humans). A recent large population based study compared pregnancy outcomes in 397 patients who underwent gadolinium contrast-enhanced MR during pregnancy with more than 1 million patients who did not undergo an MR during pregnancy. They identified that exposure to gadolinium at any time during pregnancy was associated with an increased risk of rheumatological, inflammatory, or infiltrative skin disorders as well as still birth (adjusted relative risk for still birth: 3.70; 95% CI 1.55–8.85) [4]. Despite these risks, there may be rare clinical scenarios for which the benefit of administering Gadolinium contrast outweighs the harm, including high-risk maternal conditions such as known or suspected placenta percreta, maternal malignancies (particularly of the brain and spine), or if the patient/clinical team are planning termination of pregnancy [7]. Computed tomography (CT) is rarely used in pregnancy given the risks of ionizing radiation to the developing fetus; however, CT may be indicated in the setting of maternal trauma [8] and for staging of choriocarcinoma [9].

MR imaging protocols

For dedicated placental MR imaging, a multichannel surface coil should be utilized to maximize signal. Parallel imaging techniques should also be used when possible to decrease scan time and reduce SAR [10]. Overdistension of the urinary bladder should be avoided as this may result in a false positive interpretation of placenta percreta, and may also increase patient discomfort. On the other hand, a fully collapsed urinary bladder can also make assessment of bladder invasion by placental tissue challenging [11].

Our placental MR protocol is shown in Table 1. At our institutions, we perform balanced steady state free precession (SSFP) and fast T2-weighted images (T2WI) including Half-Fourier Single Shot Turbo Spin Echo (HASTE) in the axial, sagittal, and coronal planes. These techniques demonstrate excellent soft tissue contrast between the placenta and adjacent myometrium while minimizing maternal and fetal motion. High-resolution small field of view T2WI acquisitions are often not helpful due to image degradation by uterine and respiratory motion. Images are ideally checked by the radiologist during the exam and additional oblique planes may be chosen to best delineate the placental-myometrial or placental-bladder interface in cases of suspected placental accreta spectrum disorder. T1-weighted images (T1WI) obtained as 3D gradient recall echo with fat suppression are also included to detect high signal intensity blood products [10, 11]. At our institutions, we do not use Gadolinium-based contrast agents in pregnancy; however, dynamic Gadolinium contrast-enhanced MR of the placenta continues to be investigated, as it permits quantification of placental perfusion, permeability and blood volume, and may be more accurate in the assessment of placenta accreta spectrum disorder [12–14]. Emerging techniques including arterial spin labeling MR, blood oxygen-level dependent and MR spectroscopy of the placenta provide functional information without the need for Gadolinium contrast, but these techniques are not yet validated for clinical use [15].

MR imaging findings of the normal gravid uterus, placenta and placental variants

Normal gravid uterus

The radiologist must be familiar with normal gravid uterus and placental anatomy in order to recognize different pathologic conditions. The normal gravid uterus has an inverted pear-shape with the fundus and body greater in anteroposterior dimension than the lower uterine segment. The normal uterine contour is smooth

Table 1. MR protocol for evaluation of the placenta

Imaging sequence and plane	Acquisition time (s)	TR (ms)/ TE (ms)	Flip angle (degrees)	Section thickness (mm)	Gap (mm)	Field of view (mm)	Matrix size
HASTE							
Coronal	30	1000/76	180	5	0	400 × 400	256 × 256
Axial	28	1000/76	180	5	0	261.3 × 380	176 × 256
Sagittal	25	1270/76	180	6	1.5	350 × 350	256 × 256
HASTE fat-suppressed							
Axial	30	1000/76	180	5	0	261.3 × 380	176 × 256
True FISP							
Coronal	23	4.3/2.15	80	6	1.2	350 × 350	195 × 256
Axial	19	4.3/2.15	80	6	1.2	350 × 350	195 × 256
Sagittal	19	4.3/2.15	80	6	1.2	350 × 350	195 × 256
T1-weighted fast low-angle shot 2D fat-suppressed							
Axial	46	171/2.64	70	8	2	247.5 × 330	134 × 256

Coverage is from the fundus of the uterus to below cervix

with no focal bulges. The myometrium normally exhibits a tri-layer appearance on T2WI—the middle layer is intermediate signal and is surrounded on either side by thin low signal intensity inner and outer layers (Fig. 1). The utero-placental interface is normally seen as a thin, smooth, uninterrupted and gently curved hypointense interface on T2WI and SSFP. Normal flow-voids can be seen in the retroplacental region and in the placenta, especially near the cord insertion [11]. As the fetus grows and the normal myometrium thins later in pregnancy, the tri-layer appearance may no longer be apparent.

Normal placenta

The placenta normally has a discoid shape, measuring between 2 and 4 cm in thickness, and may be located anterior, posterior, lateral, or fundal. Placental tissue grows and can migrate to different positions throughout the first 15-week gestation as placental tissue seeks preferential areas of increased blood supply (trophotropism). Abnormal thinning of the placenta can be seen with vascular and hematologic conditions while placental thickening may be due to hydrops, infection, maternal diabetes or anemia. Uterine leiomyomas and focal myometrial contractions (Fig. 2) are potential mimics of placental thickening, the latter of which are usually transient and may change or resolve completely during the course of the MR exam [16].

On T2WI and SSFP, the placenta is normally homogeneous intermediate signal, with gentle lobulations. The placenta has a fetal surface and a maternal surface. The fetal surface, also known as the chorionic plate, is the location of umbilical cord insertion. The maternal surface of the placenta contains placental

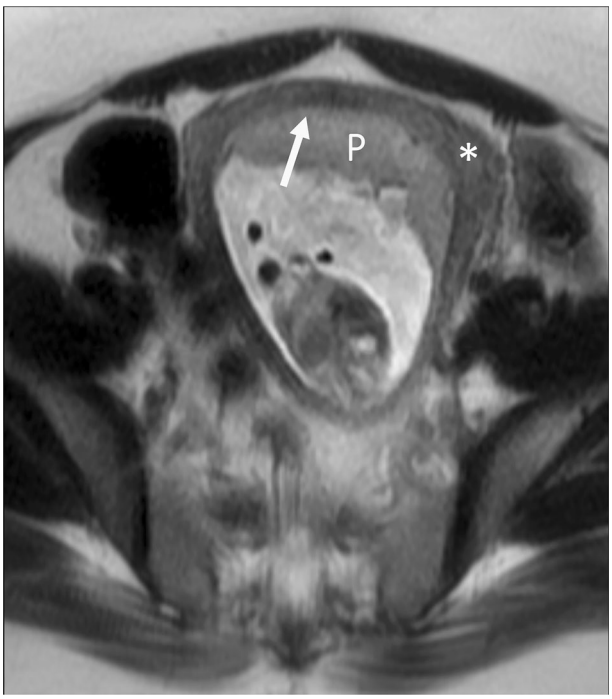

Fig. 1. Normal placenta and gravid uterus in a 26-year-old female with a 2nd trimester intrauterine pregnancy. Axial T2W MR image shows the placenta (P) located in the left anterior uterine body. Note the normal tri-layer appearance of the myometrium (asterisk)—the middle myometrial layer is T2 intermediate signal, and the inner and outer layers are thin and T2 hypointense. The utero-placental interface is T2 hypointense, thin, smooth, and uninterrupted (arrow). The tri-layer appearance of the myometrium may not be visible as the normal myometrium thins in the third trimester.

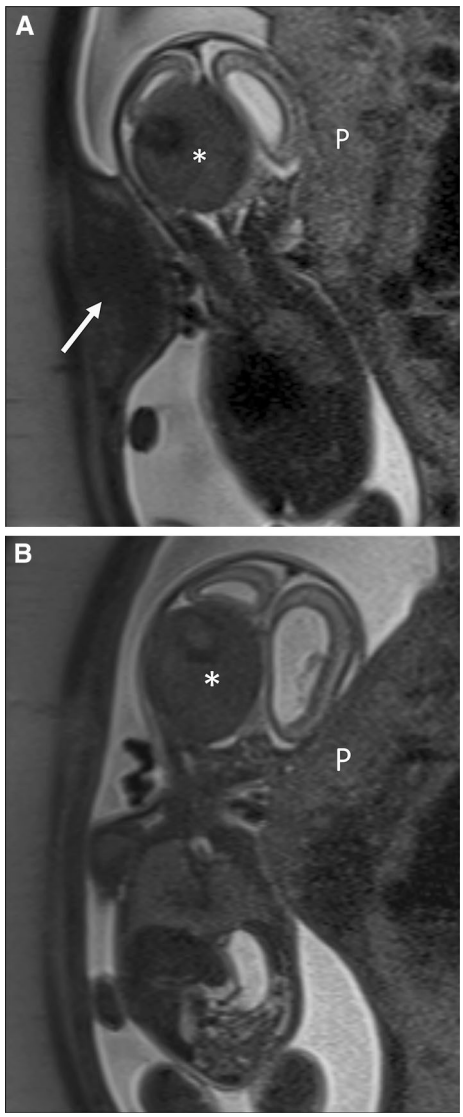

Fig. 2. Transient myometrial contraction in a 24-year-old female with a 2nd trimester intrauterine pregnancy. **A** Sagittal T2W MR image demonstrates a focal rounded area of decreased T2 signal involving the anterior uterine myometrium (arrow). Also note the large T2 hypointense fetal intracranial mass (asterisk). **B** Sagittal T2W MR image obtained later in the course of the MR exam shows that the myometrial contraction has resolved. The placenta (P) is located posteriorly.

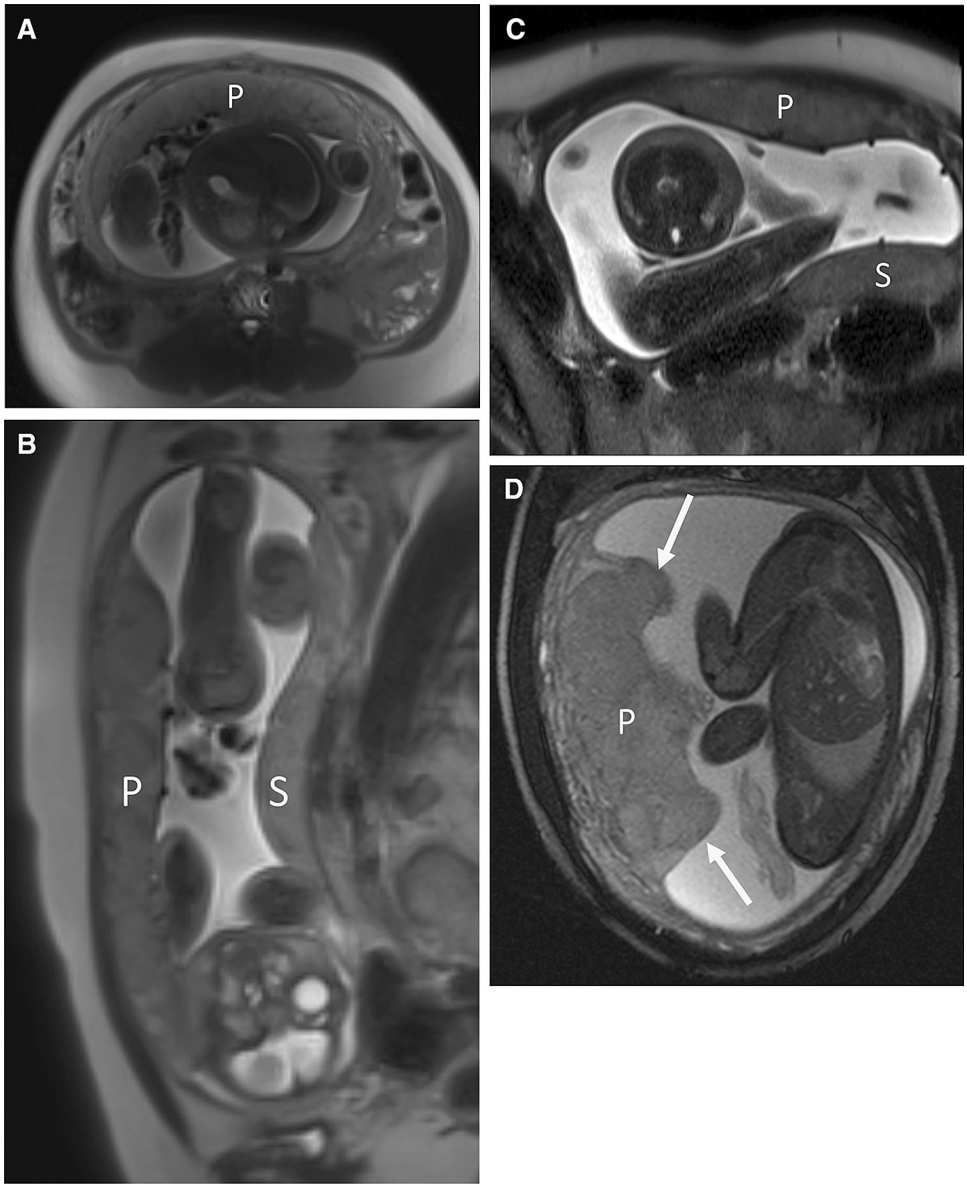

Fig. 3. Variant placental morphologies in three different patients. **A** Discoid single lobe placenta. Axial T2W MR image demonstrates discoid single lobe anteriorly located placenta (P). Single discoid morphology of placenta is the most common subtype. **B**, **C** Succenturiate placenta. Sagittal (**B**) and axial (**C**) T2W MR images show a smaller accessory placental lobe posteriorly (S) which is separate from the main disk of the anteriorly located placenta (P). **D** Circumvallate placenta. Coronal T2W MR image shows that the fetal surface (chorionic plate) of the placenta (P) is smaller than the uterine side of the placenta (basal plate) with a raised rounded ridge of placental tissue at the placental margins (arrows).

cotyledons, which are visualized on T2W images separated by thin bands of T2 hypointense signal and become more prominent with increasing gestational age. As the pregnancy progresses and the normal uterus thins, the tri-layer appearance of the uterus may not be perceivable; however, the myometrium should not demonstrate focal bulges or areas of mural disruption [11].

Placental variants

Discoid placenta is the most common placental morphology (Fig. 3A), followed by bilobed (two equal size adjacent placental lobes) and succenturiate lobes (an accessory lobe separate from the dominant placental lobe; Fig. 3B, C). Less frequently seen variants include circumvallate placenta (small chorionic plate relative to basal plate, creating a raised edge of tissue at the placental margins; Fig. 3D) and placenta membranacea

(thin membranous structure circumferentially occupying the entire periphery of the chorion) [16].

Umbilical cord insertion

The umbilical cord normally inserts centrally on the placenta (Fig. 4A) but can be marginal (inserting less than 2 cm from placental edge; Fig. 4B) or velamentous (inserting on chorioamniotic membranes rather than directly on placental tissue; Fig. 4C). The latter scenario results in umbilical vessels which extend for a variable length between the amnion and chorion and are at risk for injury because they are unprotected by Wharton's jelly [17]. Umbilical cord insertion is typically evaluated with second trimester US, but is also well seen on T2WI.

Twin gestations

Chorionicity and amnionicity of twin gestations are most often determined with US, which has a high degree of specificity and sensitivity [18], but diagnostic findings can also be seen on MR. Dichorionic-diamniotic twins are characterized by separate amniotic sacs and placentas supplying each fetus. The twin peak sign represents a triangular projection of placental tissue seen in the first trimester and is pathognomonic for dichorionic-diamniotic twins, as is a thick (≥ 2 mm) inter-twin membrane which consists of the two layers of amnion and two layers of chorion separating the fetuses [19] (Fig. 5A). Monochorionic-diamniotic twins have two amniotic sacs but share one placenta and have a thin inter-twin mem-

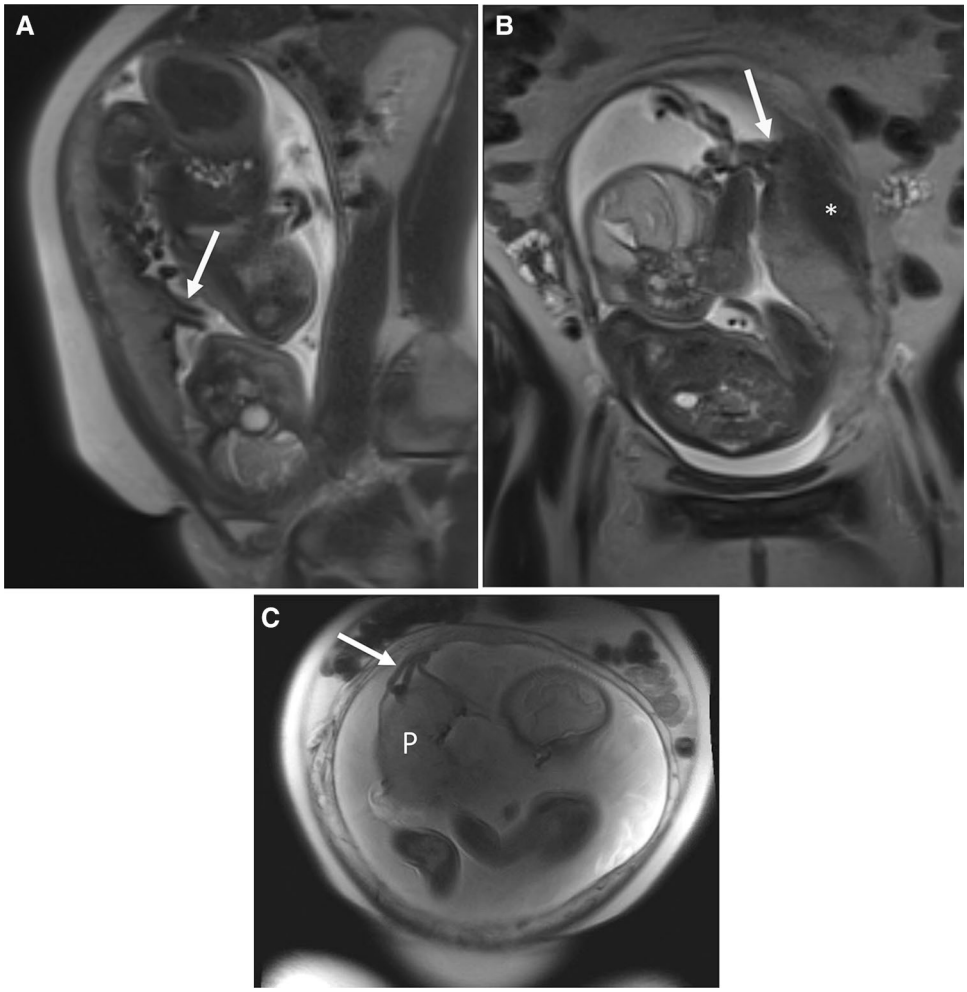

Fig. 4. Umbilical cord insertion. **A** Normal central cord insertion. Sagittal T2W MR image demonstrates the umbilical cord inserting centrally on the placental disk (arrow). **B** Marginal cord insertion. Coronal T2W MR image demonstrates the umbilical cord inserting within 2 cm of the edge of the placenta superiorly (arrow), compatible with marginal cord insertion. Low signal intensity in the subplacental zone (asterisk) was transient and not present on later sequences, compatible with a uterine contraction. **C** Velamentous cord insertion. Coronal T2W image demonstrates the umbilical vessels (arrows) inserting on chorionic membranes adjacent to the placenta (P).

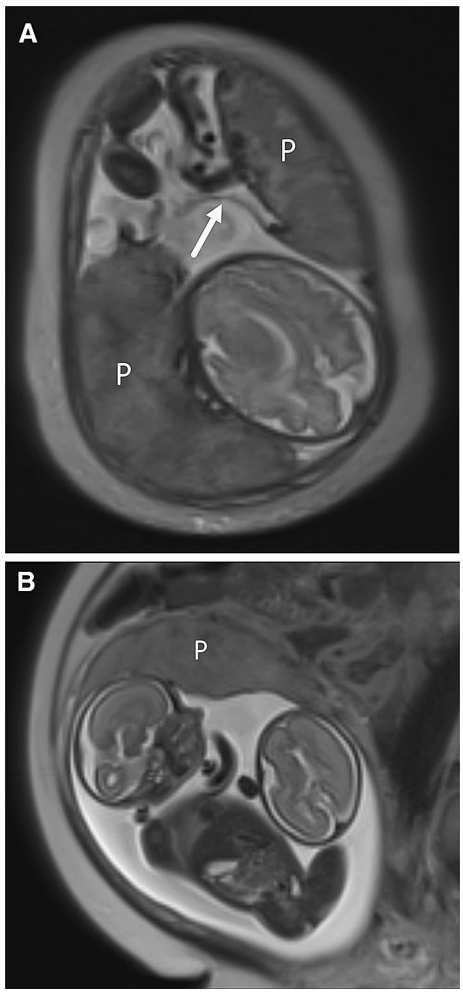

Fig. 5. MR of Twin chorionicity and amnionicity. **A** Coronal T2W MR image demonstrates two intrauterine fetuses, two placentas (P) and a thick inter-twin membrane (arrow) representing the two layers of amnion and two layers of chorion separating each fetus. **B** Monochorionic-monoamniotic twins. Sagittal T2W MR image demonstrates two intrauterine fetuses with a single placenta (P) and no inter-twin membrane, consistent with monochorionic monoamniotic twins.

brane [20]. Monochorionic-monoamniotic twins share one amnion and one placenta with no intervening membrane. Monochorionic twins may be complicated by twin–twin transfusion syndrome or twin embolization syndrome, and monoamniotic twins are at risk of cord entanglement [21] (Fig. 5B).

Uterine incarceration

Uterine incarceration is a rare complication of pregnancy in which a retropositioned gravid uterus becomes trapped in the deep pelvis between the sacral promontory and

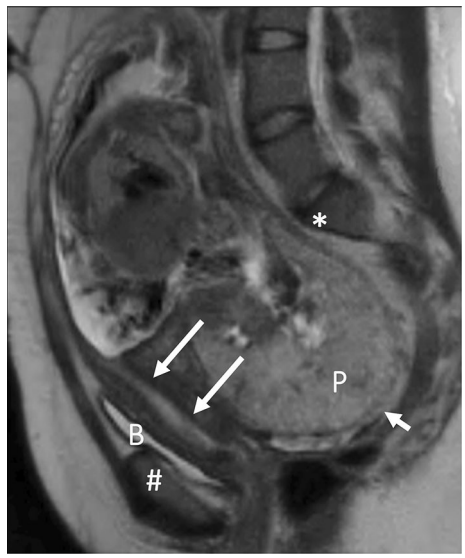

Fig. 6. Uterine incarceration in a 28-year-old female with a 3rd trimester intrauterine pregnancy. Sagittal T2W image demonstrates retroflexed anteverted uterus with the uterine fundus (short arrow) located postero-inferiorly in the deep pelvis between the sacral promontory (asterisk) and pubic symphysis (#), compatible with uterine incarceration. The cervix (long arrows) is stretched and elongated anteriorly, and the urinary bladder (B) is compressed anteriorly. The placenta (P) is located at the fundus.

pubic symphysis. The diagnosis may be suggested if physical exam shows uterine size less than expected for dates in a patient with a known retroverted uterus, but more commonly symptoms are non-specific and imaging is required to make a definitive diagnosis [22]. Uterine incarceration may be diagnosed on US, but MR, particularly images obtained in the sagittal plane, provides a more complete assessment of the relevant anatomic relationships [23]. Findings of uterine incarceration include a retropositioned uterus with the fundus located deep in the posterior pelvis inferior to the sacral promontory, a stretched elongated appearance of the cervix, and anterior displacement of the urinary bladder [24] (Fig. 6). Predisposing conditions include uterine leiomyomas, endometriosis, pelvic inflammatory disease, and variant uterine anatomy. Complications of uterine incarceration include urinary retention, constipation, intra-uterine growth restriction, uterine ischemia, premature labor and fetal death [22]. Recognizing uterine incarceration is not only important to reduce the risk of these complications, but also to prevent iatrogenic injury to the cervix, bladder, or vagina during cesarean section. In patients with known uterine incarceration, some authors have advocated a vertical cesarean incision rather than the typical low transverse incision, to minimize the risk of injury to the anteriorly displaced cervix, bladder, and vagina [25].

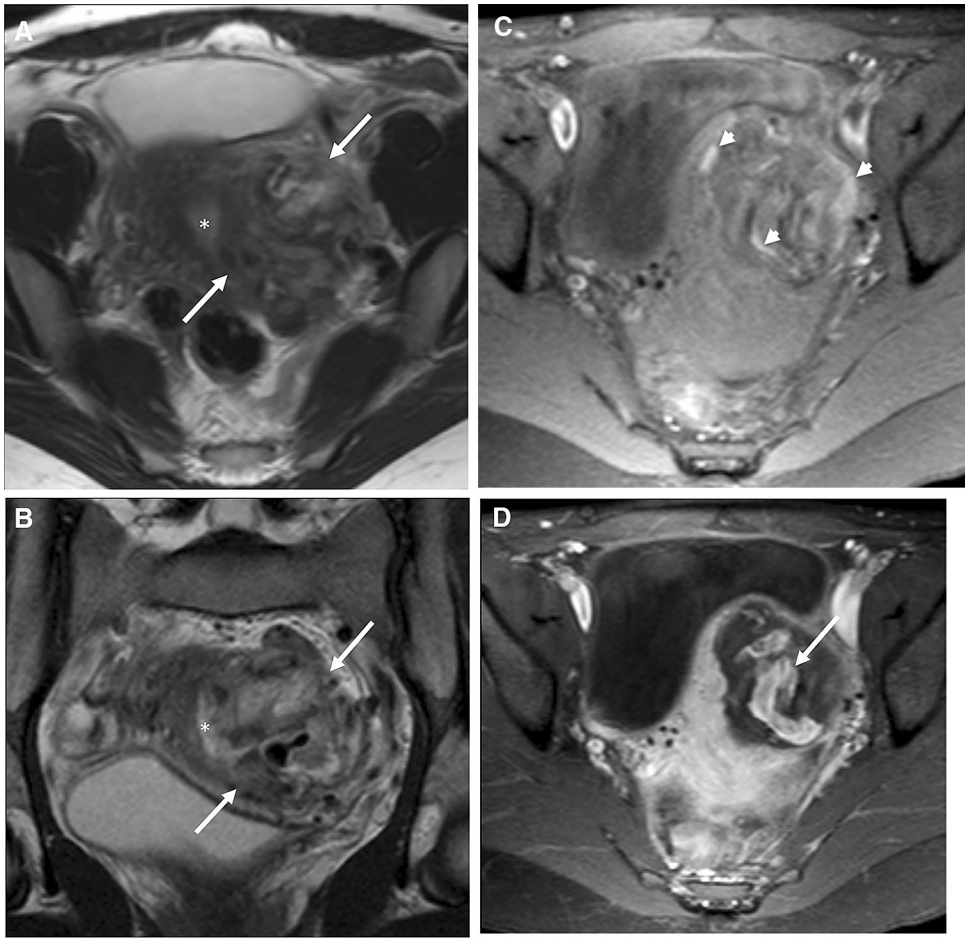

Fig. 7. Uterine rupture in a 36-year-old female with prior cesarean section. **A** Axial and **B** coronal T2W MR images demonstrate a large heterogeneous signal mass involving the left uterine wall (arrows), which communicates with the endometrial cavity (asterisk). **C** Axial T1W fat suppressed MR image demonstrates the mass contains hyperintense components (arrowheads). **D** Axial T1W fat suppressed gadolinium contrast-enhanced MR image demonstrates the mass has central regions of enhancement (arrow). βHCG was elevated. At surgery, a large c-section ectopic pregnancy with uterine rupture was found, and the patient was treated with hysterectomy.

Uterine rupture

Uterine rupture is a potentially catastrophic complication of pregnancy, defined as disruption of the uterine wall, with or without expulsion of the fetus [26]. Most uterine ruptures occur during labor. Risk factors include previous cesarean section (especially vertical/classical), trauma, uterine over distension, placenta percreta and choriocarcinoma [27]. US and MRI findings include a frank defect in the uterine wall, intrauterine and free peritoneal blood, and fetal or placental tissue located outside of the uterus [28] (Fig. 7).

Placental hemorrhage and abruption

Placental hemorrhage may occur within the placental parenchyma or adjacent to the placenta on the maternal (retroplacental) or fetal (subchorionic) surfaces (Fig. 8). The diagnosis is usually apparent on US as an avascular circumscribed mass which may be hyperechoic or hypoechoic, depending on acuity. MR signal characteristics of hemorrhage also vary depending on the acuity—acute hemorrhage is typically T1 iso-hypointense and T2 hypointense, while subacute hemorrhage is T1 hyperintense and chronic hemorrhage is T1 and T2 hypointense [29, 30].

Placental abruption represents premature separation of the placenta before delivery and is the most common cause of fetal death in cases where the mother survives, typically seen in the setting of maternal trauma [8]. Other causes of abruption include maternal vascular disease, chorioamnionitis, and cocaine use. Placental abruption and placenta previa account for more than 50% of all cases of antepartum hemorrhage [31]. The prognosis is proportional to the degree of utero-placental separation [32].

US may be the first study performed to evaluate the fetus in the setting of trauma, but sonographic findings

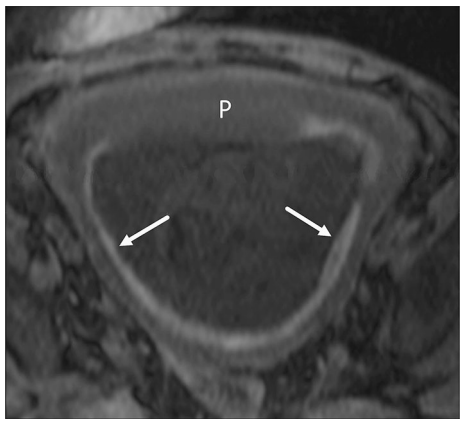

Fig. 8. Subchorionic hemorrhage in a 34-year-old patient. Axial T1W fat suppressed image demonstrates T1 hyperintense subchorionic hemorrhage surrounding approximately two-thirds of the gestational sac circumference (arrows). The placenta (P) is located anteriorly.

lack sensitivity and often do not display the full extent of the abnormality [33]. CT is indicated in pregnant patients suffering significant trauma despite the radiation risk, as it permits rapid assessment of potentially life-threatening injuries to both the mother and fetus. CT findings of placental abruption include full-thickness areas of decreased placental enhancement or retroplacental high attenuation hematoma [8, 34]. On MR, the signal intensity of placental abruption varies depending on acuity (see above), and may also be associated with blood products floating in the amniotic fluid (Fig. 9).

Placenta previa

Placenta previa occurs when placental implantation in the lower uterine segment results in partial or complete covering of the internal cervical os. Cesarean delivery is typically recommended to minimize the risk of maternal hemorrhage during labor. The inferior edge of the pla-

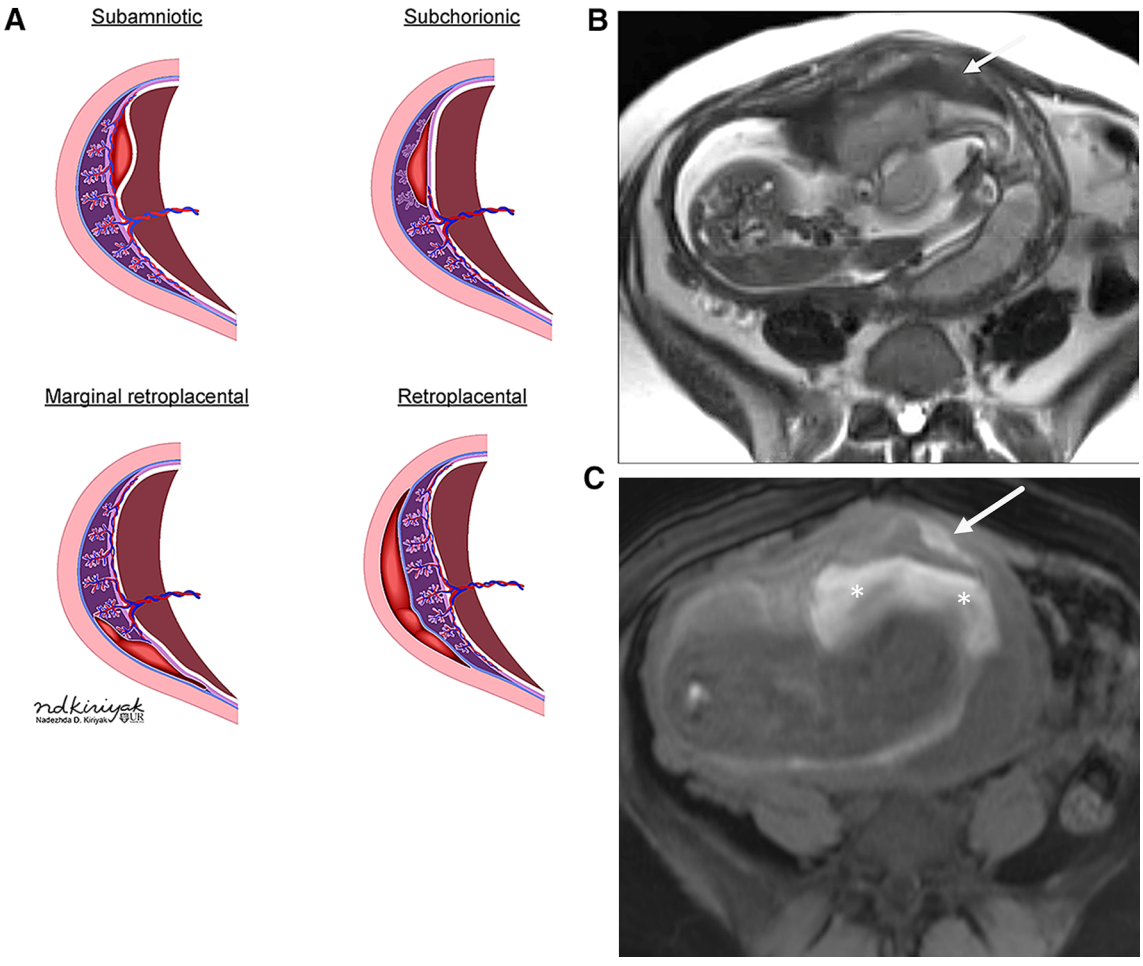

Fig. 9. Placental abruption. **A** Illustration of different locations of placental abruption. **B**, **C** Retroplacental abruption in a 28-year-old woman with a 3rd trimester intrauterine pregnancy. **B** Axial T2W MR image shows hypointense retroplacental hematoma (arrow) which was proven to represent placental abruption. **C** Axial T1W fat-suppressed image shows hyperintense retroplacental hematoma (solid arrow) and hemorrhage within the amniotic fluid (asterisks).

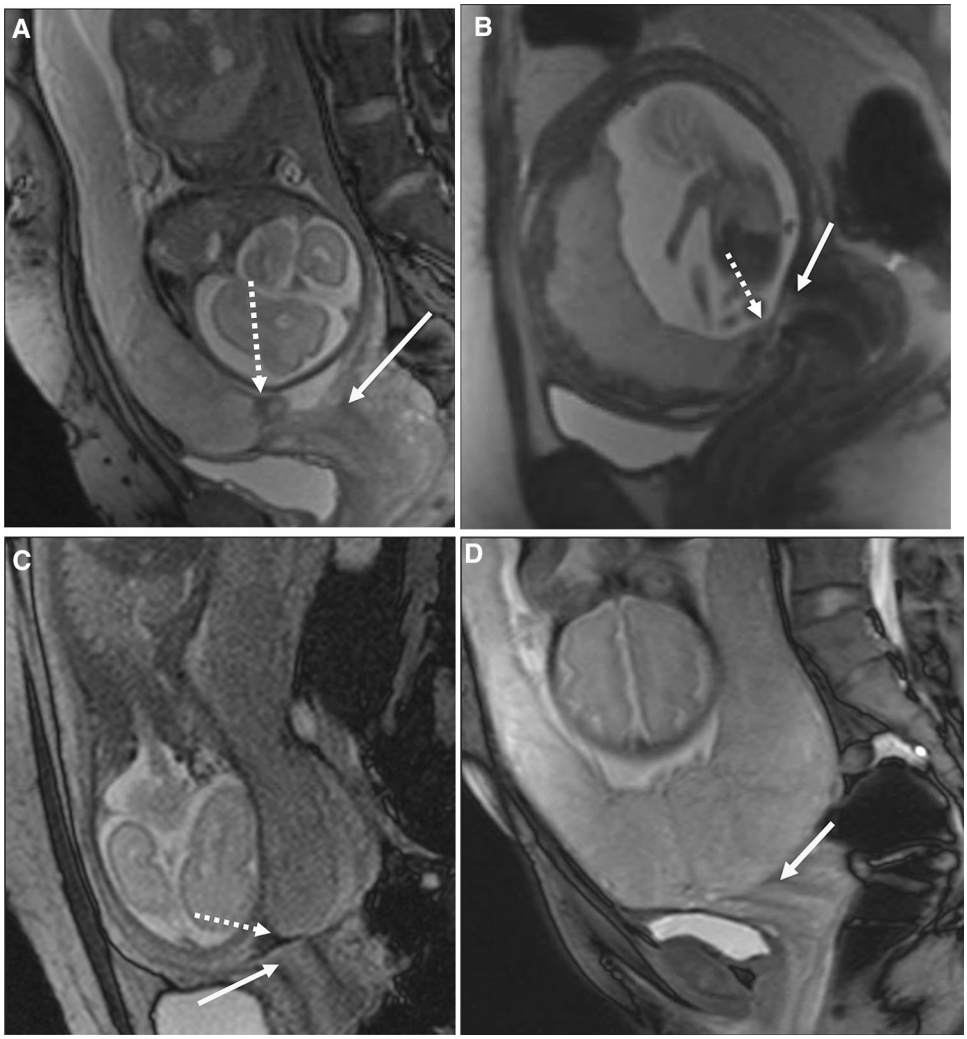

Fig. 10. Spectrum of placenta previa. **A** Low-lying placenta. Sagittal True-FISP MR image shows the inferior placental edge (dashed arrow) extends to within 2 cm of the internal cervical os (solid arrow). **B** Marginal placenta previa. Sagittal T2W MR image shows the placental edge (dashed arrow) extends to the margin but does not cover the internal os (solid arrow). **C** Partial placenta previa. Sagittal True-FISP MR image shows the placenta partially covers the internal cervical os (solid arrow). **D** Complete placenta previa. Sagittal True-FISP MR image shows the placenta completely covers the internal cervical os (solid arrow). The diagnosis of placenta previa should not be made before 15 weeks gestation because of placental trophotropism.

centa is normally located at least 2 cm from the internal cervical os after a gestational age of 15 weeks. Low-lying placenta is characterized by the lower placental margin within 2 cm of the internal os (Fig. 10A). Marginal previa is diagnosed if the placenta extends to the edge of the internal os but does not cover it (Fig. 10B). In partial placenta previa, the placenta partially covers the internal cervical os (Fig. 10C) and in complete previa, the entire internal cervical os is covered by the placenta (Fig. 10D). Due to normal trophotropism and migration of the placenta during the first trimester, a diagnosis of placenta previa should not be made until after 15 weeks gestation. Suspected cases of placenta previa seen prior to 15 weeks should be re-evaluated with US to confirm placental position prior to delivery [35]. Transvaginal US is the gold standard for imaging of placenta previa, but this condition can also be accurately diagnosed with MR. Sagittal MR images optimally display the relationship between the placenta and internal os to evaluate for placenta previa. An important pitfall is an over-distended urinary bladder which can compress the lower uterine segment and result in a false positive diagnosis of placenta previa [36].

Vasa previa

Vasa previa represents fetal vessels crossing the internal cervical os. It is associated with low-lying placenta, placenta previa, variant placental morphology, and twin gestations. The vessels are unprotected by Wharton's

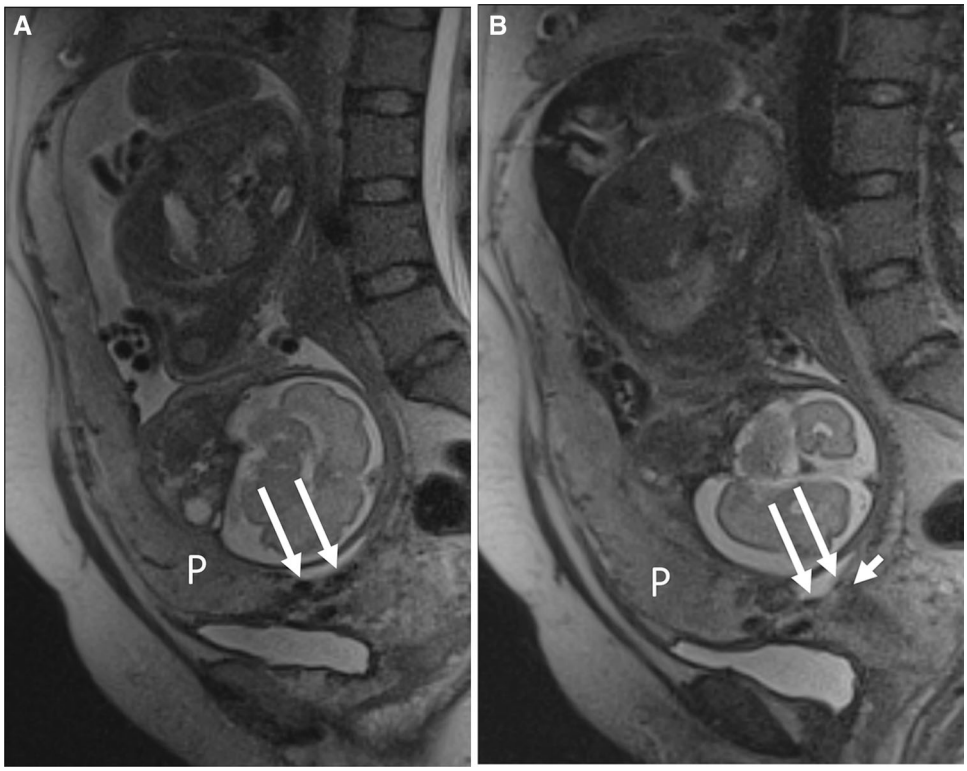

Fig. 11. Vasa previa in the 29-year-old female with a 3rd trimester intrauterine pregnancy. Para-midline sagittal T2W images obtained on two adjacent slices (**A**, **B**) demonstrate a low-lying anteriorly located placenta (P) and several hypointense flow voids (arrows) extending from the inferior placental margin covering the internal cervical os (arrowhead in **B**).

jelly and are prone to injury during rupture of membranes and delivery, which can result in fetal hemorrhage and death [37, 38]. The diagnosis of vasa previa is commonly made with Doppler US, demonstrating fetal vessels covering the internal os, but findings may also be seen on MR (Fig. 11). Flow voids overlying the internal os may be seen on T2WI, and time-of-flight sequences can demonstrate the direction of flow within the umbilical vessels [39].

Placental accreta spectrum disorder

Placenta accreta vera, placenta increta, and placenta percreta represent a continuum under the broader category of placental accreta spectrum disorder (PAD). In placenta accreta vera, chorionic villi attach to but do not invade myometrial tissue. In placenta increta, villi invade partially though the myometrium (Fig. 12), and in the most severe form, placenta percreta, villi penetrate through the entire myometrial thickness and may extend through the serosa into adjacent structures [40] (Fig. 13). Failure of complete placental detachment in patients with PAD can cause life-threatening maternal hemorrhage at the time of placental separation, which may result in disseminated intravascular coagulopathy, adult respiratory distress syndrome or even death. Therefore, antepartum diagnosis and localization of PAD is crucial

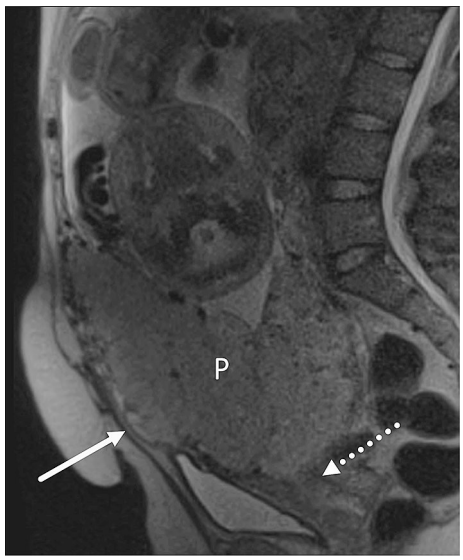

Fig. 12. Placenta increta in a 25-year-old woman with a 3rd trimester intrauterine pregnancy. Sagittal T2W image demonstrates focal bulge of the lower uterine segment (solid arrow) with marked thinning of the adjacent uterine myometrium, thickening and heterogeneous signal in the placenta (P). There is no extension of placental tissue to the uterine serosa. Placenta increta was confirmed at surgery. Note that complete placenta previa is also present (dotted arrow).

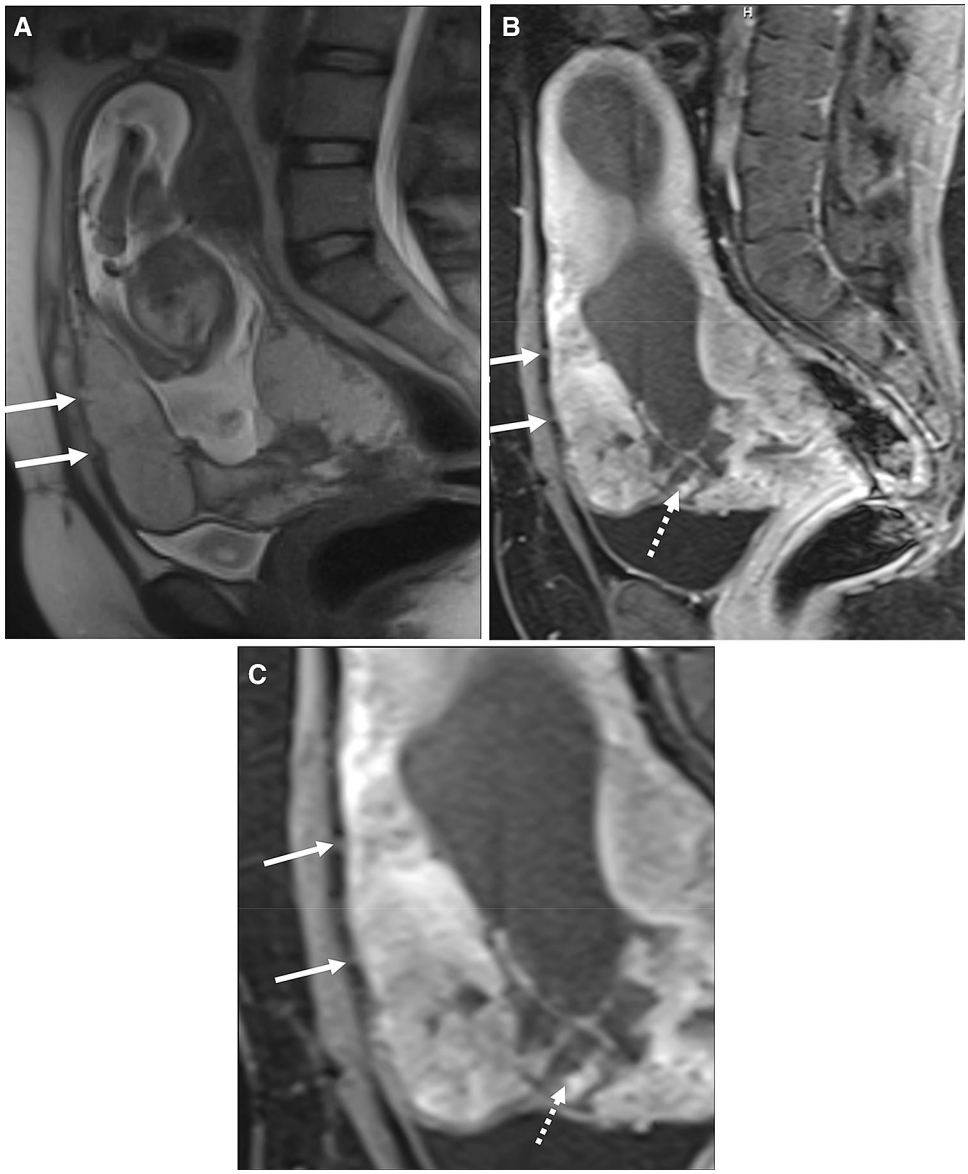

Fig. 13. Placenta percreta in a 30-year-old female with a 3rd trimester intrauterine pregnancy with anencephaly. Sagittal T2W (**A**) and T1W Fat suppressed gadolinium contrast-enhanced (**B**) MR images demonstrate abnormal bulging of the lower uterine segment. Placental tissue focally extends beyond the uterine serosa into the properitoneal fat (solid arrows). These findings are better seen on the magnified image of Fig. 13B (**C**). There is also complete placenta previa and hypoenhancement of the placenta at the lower uterine segment compatible with placental infarct (dashed arrow). Placenta percreta was confirmed during surgery at which time the urinary bladder was also found to be invaded with placental tissue, requiring partial cystectomy at the time of hysterectomy.

as it may alter surgical approach and reduce fetal and maternal morbidity and mortality.

Prior cesarean delivery is a recognized risk factor for PAD, believed to be related to deficiency of the decidua basalis at the site of cesarean scar, and as the rate of cesarean section continues to rise, the incidence of PAD is also increasing [41, 42]. Placenta previa is also a risk factor for PAD. Additional but less strongly associated predisposing factors include advanced maternal age, congenital uterine anomalies, prior dilation and curettage or myomectomy. Studies in the United States and abroad suggest the prevalence of PAD may be as high as 1 in 500 deliveries [43].

US features of PAD include loss of the normal retroplacental clear space, irregularity of the bladder wall with increased vascularity, thinning of the myometrium < 1 mm, and prominent placental lacunae with ill-defined margins, irregular shape and turbulent flow [44]. At our institutions, if an abnormality suggestive of PAD is seen on US, most patients will be referred for MR.

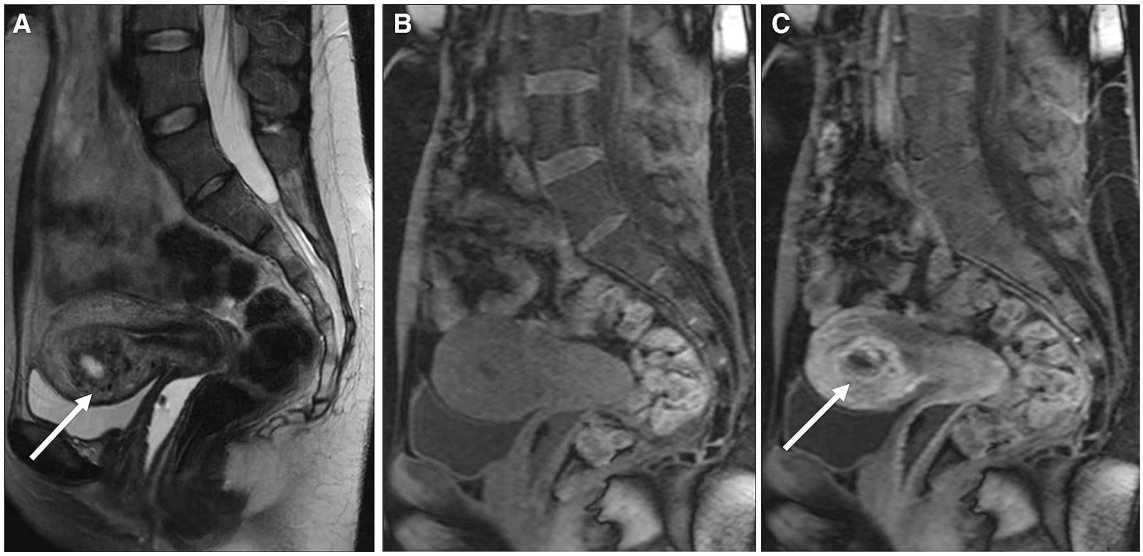

Fig. 14. Invasive mole in a 30-year-old female with markedly elevated βHCG. Sagittal T2W (**A**), T1W fat suppressed pre-contrast (**B**) and T1W fat suppressed post-gadolinium contrast-enhanced (**C**) MR images demonstrate a heterogeneous centrally T2 hyperintense mass with peripheral areas of enhancement, located in the endometrium of the ventral uterine body/fundus with invasion of the adjacent myometrium (arrows). Pathology demonstrated findings consistent with invasive hydatiform mole.

On MR, findings of PAD include focal bulging of the placenta, creating an hour-glass configuration of the uterus when viewed in the sagittal plane, rather than the normal inverted-pear shape. Another finding suggestive of PAD is disruption of the myometrial-placental interface, with loss of the normal smooth thin arc of T2 hypointense tissue, akin to loss of the retroplacental clear space seen on US. Additional findings include prominent T2 hypointense intraplacental bands which are irregular and thicker than the thin regularly spaced septa frequently seen in normal third trimester gestations [11, 16]. While some authors believe that administration of gadolinium contrast can improve the accuracy of diagnosing PAD [12–14], we do not utilize gadolinium in pregnancy for this purpose. If placental tissue is seen to frankly extend through the myometrium and invade other structures, the diagnosis of placenta percreta can be confidently made. However, in practice, it can be very challenging to distinguish between different subtypes of PAD when there is no obvious bladder invasion or extrauterine placental extension.

Gestational trophoblastic disease

Gestational trophoblastic disease (GTD) is a category which includes partial and complete hydatidiform moles, invasive mole and choriocarcinoma. Patients usually present with first-trimester bleeding, large-for-date uterine size and hyperemesis. Laboratory analysis will show markedly elevated β-human chorionic gonadotropin (β-hCG) [9].

Complete molar pregnancy is the most common form of GTD and occurs following fertilization of an empty ovum, resulting in proliferation of trophoblastic tissue and a complex multicystic mass. Sonographically, the typical appearance is a large heterogeneous endometrial mass with numerous variably-sized cysts and no apparent fetal parts, producing a cluster of grapes appearance [45]. Partial hydatidiform mole is less common and results from fertilization of a normal ovum by two sperm, resulting in a triploid genotype. On US, the appearance can resemble that of a complete mole, but unlike complete moles, fetal tissue is also present. MR is not performed to distinguish between partial or complete moles, but may be obtained to determine if there is an invasive component, as evidenced by molar tissue extending into the myometrium (Fig. 14). Invasive mole may occasionally demonstrate deep invasion with extension through the uterus into the peritoneum [9]. A highly vascular process, GTD demonstrates avid enhancement, heterogeneous signal on T2WI, and may have areas of hemorrhage and cystic change [46]. In contradistinction to invasive moles, which are locally aggressive but not malignant, choriocarcinomas are malignant neoplasms and frequently metastasize to the lungs. MR is useful in determining depth of invasion of both invasive mole and choriocarcinoma, but cannot reliably distinguish between these two entities [9].

Retained products of conception

Retained products of conception (RPOC) is usually suspected clinically when examination reveals an incomplete placenta after delivery, miscarriage or termination of pregnancy. US findings of RPOC are nonspecific but include heterogeneous echogenicity material

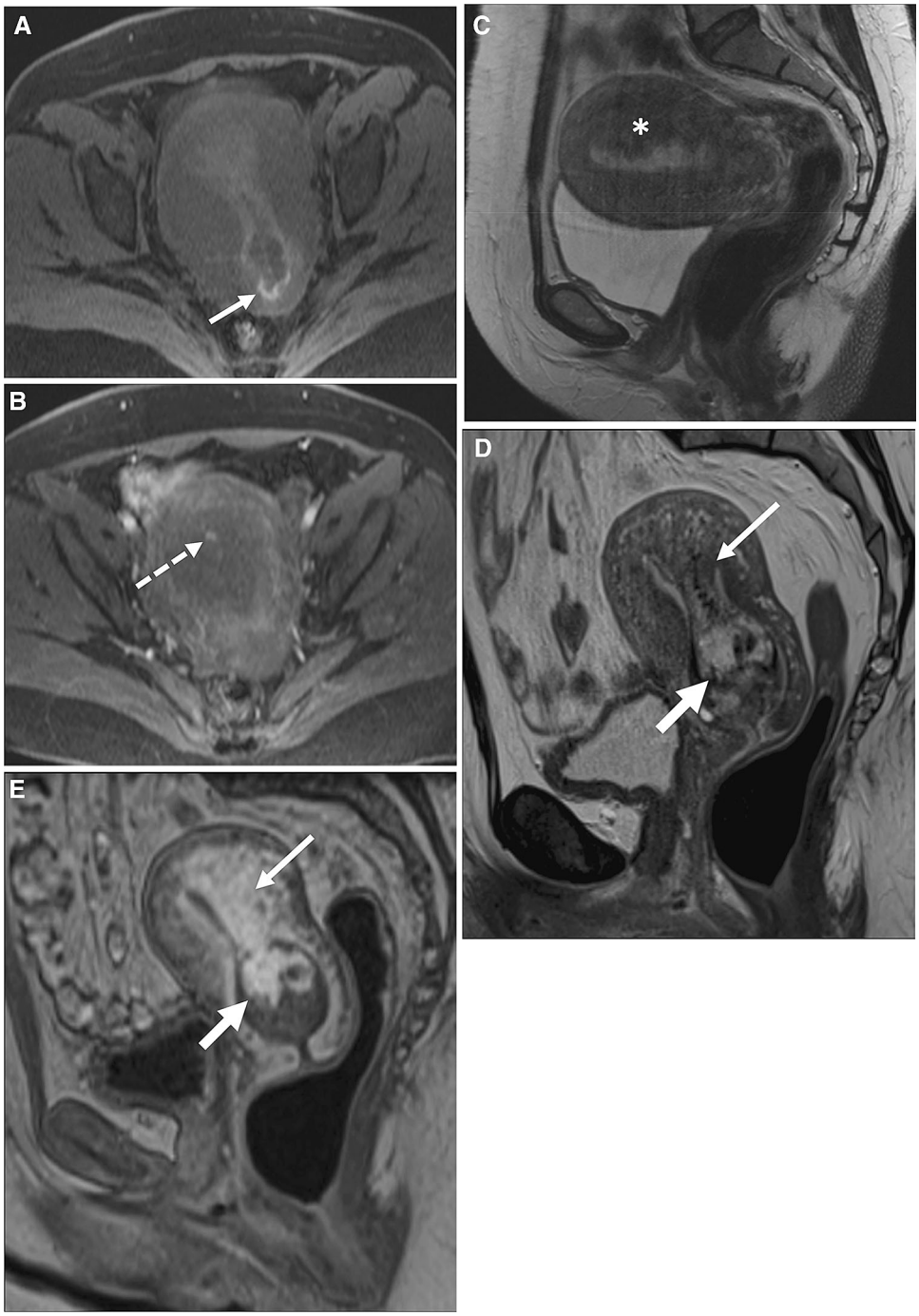

Fig. 15. Retained products of conception. 38-year-old female status post spontaneous vaginal delivery with RPOC (**A**–**C**). Axial T1W fat suppressed (**A**), axial gadolinium contrast-enhanced fat suppressed T1W (**B**) and sagittal T2W MR images (**C**) demonstrate intrinsic T1 hyperintense signal material within the endometrial cavity compatible with blood products (arrow) and poorly defined T2 hypointense signal material involving the endometrium and myometrium of the posterior uterine fundus/body (asterisk). There are also a few scattered small nodular areas of post contrast enhancement (dashed arrow). RPOC in a different patient, aged 23 years status post spontaneous vaginal delivery (**D**, **E**). Sagittal T2W (**D**) and T1W gadolinium contrast-enhanced (**E**) MR images demonstrate heterogeneous T2 signal with corresponding contrast enhancement centered in the endometrium with extension to the myometrium of the fundus and posterior uterine body (thin arrow), as well as a stalk-like component of enhancing tissue extending into the endometrial cavity which distends the endometrial canal (thick arrow).

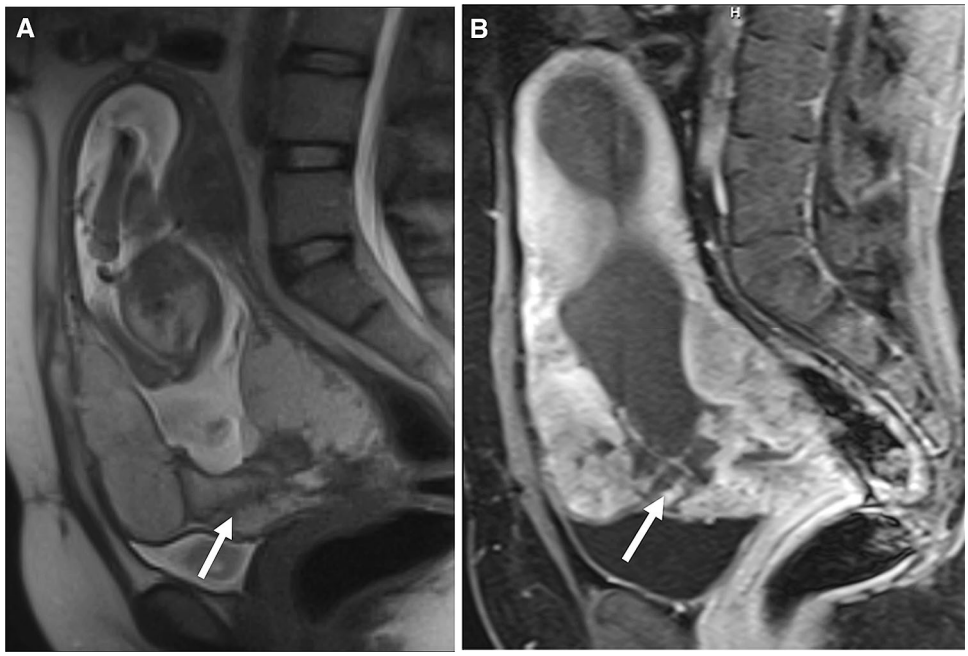

Fig. 16. Placental infarct in a 26-year-old female with placenta percreta, placenta previa and known anencephalic fetus (same case as Fig. 13). Sagittal T2W MR image (**A**) shows complete placenta previa with heterogeneous hypointense signal in the portion of the placenta covering the internal os and lower uterine segment (arrow). Sagittal T1W fat suppressed gadolinium contrast-enhanced MR image (**B**) demonstrates hypoenhancement of this portion of the placenta, compatible with infarction. Also note changes compatible with placenta percreta anteriorly, described in detail in Fig. 13.

in the endometrial canal which may have associated Doppler flow [47]. On MR, findings of RPOC include an endometrial mass of heterogeneous T2 signal, areas of T1 hyperintense blood products and post contrast enhancement [48] (Fig. 15). While the imaging appearance is non-specific and overlaps with that of GTD, the clinical scenario is often different, and β-hCG is usually only mildly elevated or normal. An additional differential diagnostic consideration is uterine arteriovenous malformation (AVM), which may develop following dilation and curettage, however uterine AVM shows characteristic flow voids, enhancing serpentine vessels on MR angiography and may demonstrate areas of susceptibility artifact [49].

Placental infarct

Placental infarction refers to ischemic villous necrosis. Small infarctions at the periphery of the placenta and involving less than 5% of the villous parenchymal volume are relatively common (up to 25% of normal pregnancies) and generally of no clinical significance. However, larger central infarctions may result in placental insufficiency, intrauterine growth restriction and fetal death [50]. Placental infarction is associated with placental abruption, advanced maternal age, maternal diabetes, hypertension, pre-eclampsia and systemic lupus erythematosus. On grayscale US, many placental infarctions are isoechoic to normal placenta and may be difficult to identify [51], although the presence of high resistance flow on spectral Doppler interrogation of the uterine arteries is indicative of placental dysfunction and should prompt further investigation as to the cause [52]. On MR, placental infarcts are hypointense on T2W images and if Gadolinium contrast is administered, are hypoenhancing compared to adjacent viable placental tissue [53] (Fig. 16).

Benign placental lesions

Placental cysts are usually small and incidental, occur at the fetal surface of the placenta near the cord insertion, and are anechoic without internal Doppler flow on US [54]. They follow fluid signal on MR and do no demonstrate enhancement. Placental venous lakes represent prominent intervillous spaces, appear hypoechoic or anechoic on US, and are usually of little clinical significance when < 2 cm, solitary or few in number [16]. Chorioangioma is the most common benign placental tumor, occurring in less than 1% of pregnancies. On US, chorioangioma appears as a solid well-circumscribed variable echogenicity mass with internal Doppler flow, often located near the cord insertion on the fetal side of the placenta. These lesions are usually asymptomatic and identified incidentally on US, however, multiple lesions or lesions larger than 5 cm have been associated with poor fetal outcomes [55]. MR is not usually performed to characterize chorioangiomas, but they show T2 hyper-

intense and T1 isointense signal, with areas of T1 hyperintense material representing hemorrhage [56].

Placental metastasis

Metastases to the placenta are very rare, believed to occur via hematogenous dissemination with deposition in the intervillous space of the placenta. Melanoma is the most common primary malignancy to metastasize to the placenta, with less frequent primary sites including lung, breast, gastric, and gynecologic neoplasms [57]. The appearance has not been well described in the radiology literature but could be included in the differential diagnosis of multiple solid placental lesions in the appropriate clinical context.

Conclusion

MRI is being utilized with increasing frequency and has many advantages compared with sonography for evaluating the placenta and gravid uterus. MR provides valuable information about the fetus, uterus, placenta, and a detailed assessment of maternal pelvic anatomy. Radiologists should be aware of the spectrum of normal placental variants, as well as benign and life-threatening conditions affecting the placenta and gravid uterus to optimize patient care and minimize fetal and maternal perinatal complications.

Compliance with ethical standards

Disclosures All authors claim no conflicts of interest or disclosures.

References

1. Hertzberg B, Middleton W, Middleton W (2015) *Ultrasound: the requisites*. Philadelphia: Elsevier
2. American College of Radiology (ACR), Society for Pediatric Radiology (SPR) (2015) ACR-SPR practice guideline for the safe and optimal performance of fetal magnetic resonance imaging (MRI). Reston: American College of Radiology (ACR), pp. 4–5. https://www.acr.org/-/media/ACR/Files/Practice-Parameters/mr-fetal.pdf?la=en
3. Kanal E, Barkovich AJ, Bell C, et al. (2013) ACR guidance document on MR safe practices: 2013. J Magn Reson Imaging 37(3):501–530
4. Ray JG, Vermeulen MJ, Bharatha A, Montanera WJ, Park AL (2016) Association between MRI exposure during pregnancy and fetal and childhood outcomes. JAMA 316:952–961
5. Hand JW, Li Y, Thomas EL, Rutherford MA, Hajnal JV (2006) Prediction of specific absorption rate in mother and fetus associated with MRI examinations during pregnancy. Magn Reson Med 55(4):883–893
6. ACR (American College of Radiology) (2017) ACR manual on contrast media version 10.3. https://www.acr.org/-/media/ACR/Files/Clinical-Resources/Contrast_Media.pdf
7. Doyle S, Messiou C, Rutherford JM, Dineen RA (2009) Cancer presenting during pregnancy: radiological perspectives. Clin Radiol 64(9):857–871
8. Raptis CA, Mellnick VM, Raptis DA, et al. (2014) Imaging of trauma in the pregnant patient. Radiographics 34(3):748–763
9. Shaaban AM, Rezvani M, Haroun RR, et al. (2017) Gestational trophoblastic disease: clinical and imaging features. RadioGraphics 37(2):681–700
10. Prayer D, Brugger PC, Prayer L (2004) Fetal MRI: techniques and protocols. Pediatr Radiol 34:685–693
11. Leyendecker JR, DuBose M, Hosseinzadeh K, et al. (2012) MRI of pregnancy-related issues: abnormal placentation. AJR Am J Roentgenol 198(2):311–320
12. Palacios Jaraquemada JM, Bruno C (2000) Gadolinium enhanced MR imaging in the differential diagnosis of placenta accreta and placenta percreta. Radiology 216:610–611
13. Tanaka YO, Sohda S, Shigemitsu S, Niitsu M, Itai Y (2001) High temporal resolution dynamic contrast MRI in a high risk group for placenta accreta. Magn Reson Imaging 19:635–642
14. Millischer AE, Deloison B, Silvera S, et al. (2017) Dynamic contrast enhanced MRI of the placenta: a tool for prenatal diagnosis of placenta accreta? Placenta 53:40–47
15. Siauve N, Chalouhi GE, Deloison B, et al. (2015) Functional imaging of the human placenta with magnetic resonance. Am J Obstet Gynecol 213(4 Suppl):S103–S114
16. Elsayes KM, Trout AT, Friedkin AM, et al. (2009) Imaging of the placenta: a multimodality pictorial review. Radiographics 29(5):1371–1391
17. Benirschke K, Kaufmann P (2000) *Pathology of the human placenta*. New York: Springer Verlag
18. Lee YM, Cleary-Goldman J, Thaker HM, Simpson LL (2006) Antenatal sonographic prediction of twin chorionicity. Am J Obstet Gynecol 195(3):863–867
19. Trop I (2001) The twin peak sign. Radiology 220(1):68–69
20. Nair M, Kumar G (2009) Uncomplicated monochorionic diamniotic twin pregnancy. J Obstet Gynaecol 29(2):90–93
21. Dias T, Mahsud-dornan S, Bhide A, et al. (2010) Cord entanglement and perinatal outcome in monoamniotic twin pregnancies. Ultrasound Obstet Gynecol 35(2):201–204
22. Gardner CS, Jaffe TA, Hertzberg BS, Javan R, Ho LM (2013) The incarcerated uterus: a review of MRI and ultrasound imaging appearances. AJR Am J Roentgenol 201(1):223–229
23. van Beekhuizen HJ, Bodewes HW, Tepe EM, et al. (2003) Role of magnetic resonance imaging in the diagnosis of incarceration of the gravid uterus. Obstet Gynecol 102:1134–1137
24. Fernandes DD, Sadow CA, Economy KE, Benson CB (2012) Sonographic and magnetic resonance imaging findings in uterine incarceration. J Ultrasound Med 31:645–650
25. Gottschalk EM, Siedentopf JP, Schoenborn I, et al. (2008) Prenatal sonographic and MRI findings in a pregnancy complicated by uterine sacculation: case report and review of the literature. Ultrasound Obstet Gynecol 32:582–586
26. Plauche W, VonAlmen W, Muller R (1984) Catastrophic uterine rupture. Obstet Gynecol. 64:792–793
27. Claydon CS, Pernoll ML (2003) Third-trimester vaginal bleeding. In: DeCherney AH, Nathan L (eds) *Current obstetric and gynaecologic diagnosis and treatment*, 9th edn. New York: Lange/McGraw Hill, pp 354–368
28. Bedi DG, Solomon A, Winsett MZ, Fagan CJ, Kumar R (1986) Ruptured uterus: sonographic diagnosis. J Clin Ultrasound 14:529–533
29. Trop I, Levine D (2001) Hemorrhage during pregnancy: sonography and MR imaging. AJR Am J Roentgenol 176(3):607–615
30. Masselli G, Brunelli R, Di Tola M, Anceschi M, Gualdi G (2011) MR imaging in the evaluation of placental abruption: correlation with sonographic findings. Radiology 259(1):222–230
31. Sinha P, Kuruba N (2008) Ante-partum haemorrhage: an update. J Obstet Gynaecol 28:377–381
32. Ananth CV, Berkowitz GS, Savitz DA, Lapinski RH (1999) Placental abruption and adverse perinatal outcomes. JAMA 282(17):1646–1651
33. Glantz C, Purnell L (2002) Clinical utility of sonography in the diagnosis and treatment of placental abruption. J Ultrasound Med 21(8):837–840
34. Wei SH, Helmy M, Cohen AJ (2009) CT evaluation of placental abruption in pregnant trauma patients. Emerg Radiol 16(5):365–373
35. Reddy UM, Abuhamad AZ, Levine D, Saade GR, Fetal Imaging Workshop Invited Participants (2014) Fetal imaging: executive summary of a Joint Eunice Kennedy Shriver National Institute of Child Health and Human Development, Society for Maternal-Fetal Medicine, American Institute of Ultrasound in Medicine, American College of Obstetricians and Gynecologists, American College of Radiology, Society for Pediatric Radiology, and Society of Radi-

ologists in Ultrasound Fetal Imaging Workshop. Am J Obstet Gynecol. 210(5):387–397
36. Dashe JS, Mcintire DD, Ramus RM, et al. (2002) Persistence of placenta previa according to gestational age at ultrasound detection. Obstet Gynecol 99:692–697
37. Catanzarite V, Maida C, Thomas W, et al. (2001) Prenatal sonographic diagnosis of vasa previa: ultrasound findings and obstetric outcomes in ten cases. Ultrasound Obstet Gynecol 17:109–115
38. Kulkarni A, Powel J, Aziz M, et al. (2018) Vasa previa: prenatal diagnosis and outcomes: thirty-five cases from a single maternal-fetal medicine practice. J Ultrasound Med 37:1017–1024
39. Oyelese Y, Jha RC, Moxley MD, Collea JV, Queenan JT (2003) Magnetic resonance imaging of vasa praevia. BJOG. 110(12):1127–1128
40. ACOG Committee on Obstetric Practice (2002) ACOG Committee opinion. Number 266, January 2002: placenta accreta. Obstet Gynecol 99(1):169–170
41. Tantbirojn P, Crum CP, Parast MM (2008) Pathophysiology of placenta acreta: the role of decidua and extravillous trophoblast. Placenta 29:639–645
42. Hull AD, Moore TR (2011) Multiple repeat cesareans and the threat of placenta accreta: incidence, diagnosis, management. Clin Perinatol 38:285–296
43. Wu S, Kocherginsky M, Hibbard JU (2005) Abnormal placentation: twenty-year analysis. Am J Obstet Gynecol 192:1458–1461
44. Baughman WC, Corteville JE, Shah RR (2008) Placenta accreta: spectrum of US and MR imaging findings. Radiographics 28(7):1905–1916
45. Benson CB, Genest DR, Bernstein MR, et al. (2000) Sonographic appearance of first trimester complete hydatidiform moles. Ultrasound Obstet Gynecol 16(2):188–191
46. Barton JW, McCarthy SM, Kohorn EI, Scoutt LM, Lange RC (1993) Pelvic MR imaging findings in gestational trophoblastic disease, incomplete abortion, and ectopic pregnancy: are they specific? Radiology 186(1):163–168
47. Kamaya A, Petrovitch I, Chen B, Frederick CE, Jeffrey RB (2009) Retained products of conception: spectrum of color Doppler findings. J Ultrasound Med 28(8):1031–1041
48. Noonan JB, Coakley FV, Qayyum A, et al. (2003) MR imaging of retained products of conception. AJR Am J Roentgenol 181(2):435–439
49. Nagayama M, Watanabe Y, Okumura A, et al. (2002) Fast MR imaging in obstetrics. Radiographics 22(3):563–580 (discussion 580–582)
50. Fox HF, Sebire N (2007) *Pathology of the placenta*. Philadelphia: Elsevier
51. Callen PW (2008) *Ultrasonography in obstetrics and gynecology*. Philadelphia: Elsevier
52. Yagel S, Anteby EY, Shen O, et al. (1999) Placental blood flow measured by simultaneous multigate spectral Doppler imaging in pregnancies complicated by placental vascular abnormalities. Ultrasound Obstet Gynecol 14:262–266
53. Malian V, Lee JH (2001) MR imaging and MR angiography of an abdominal pregnancy with placental infarction. AJR Am J Roentgenol 177(6):1305–1306
54. Brown DL, DiSalvo DN, Frates MC, Davidson KM, Genest DR (2002) Placental surface cysts detected on sonography: histologic and clinical correlation. J Ultrasound Med 21(6):641–646
55. Kung FT, Chen WJ, Hsu PH, et al. (1997) Large chorioangioma: antenatal color-flow Doppler ultrasonic imaging and its correlation with postpartum pathology, experience of 2 cases. Acta Obstet Gynecol Scand 76:277–279
56. Kawamoto S, Ogawa F, Tanaka J, Ban S, Heshiki A (2000) Chorioangioma: antenatal diagnosis with fast MR imaging. Magn Reson Imaging 18(7):911–914
57. Dildy GA, Moise KJ, Carpenter RJ, Klima T (1989) Maternal malignancy metastatic to the products of conception: a review. Obstet Gynecol Surv 44(7):535–540